Chemistry on quantum computers with virtual quantum subspace expansion

Miroslav Urbanek,* Daan Camps, Roel Van Beeumen, and Wibe A. de Jong
Computational Research Division, Lawrence Berkeley National Laboratory, Berkeley, CA 94720, USA

Several novel methods for performing calculations relevant to quantum chemistry on quantum computers have been proposed but not yet explored experimentally. Virtual quantum subspace expansion [T. Takeshita *et al.*, Phys. Rev. X **10**, 011004 (2020)] is one such algorithm developed for modeling complex molecules using their full orbital space and without the need for additional quantum resources. We implement this method on the IBM Q platform and calculate the potential energy curves of the hydrogen and lithium dimers using only two qubits and simple classical post-processing. A comparable level of accuracy would require twenty qubits with previous approaches. We also develop an approach to minimize the impact of experimental noise on the stability of a generalized eigenvalue problem that is a crucial component of the algorithm. Our results demonstrate that virtual quantum subspace expansion works well in practice.

I. INTRODUCTION

It is expected that major applications of quantum computing will be in quantum chemistry [1]. Typical chemistry problems are to find the ground state energy of a molecule, its excited states, or to extract reduced density matrices that can be used to compute various molecular properties relevant to science and industry. Traditional quantum algorithms, for example quantum phase estimation (QPE) [2], require circuit depths that are beyond the abilities of currently available quantum computers. A lot of effort has been invested into alternative approaches, most notably into the variational quantum eigensolver (VQE) algorithm [3, 4]. VQE is an iterative and hybrid quantum-classical method, where one creates a parametrized trial wave function on a quantum computer, measures observables that correspond to Hamiltonian terms of the studied molecule, estimates the electronic energy, and optimizes the set of wave-function parameters for the next iteration. It has been demonstrated that VQE can find the ground-state energy of small molecules [3, 5–12].

While the ground-state energy is an important property of a molecular configuration, the energy of excited states is even more important. Extensions of VQE have been proposed that target excited states [13, 14]. The quantum subspace expansion (QSE) algorithm [15] can extract the energy of excited states and was also found to improve the ground-state energy estimate [8, 16]. Using this method, one first creates the ground-state wave function on a quantum computer and then performs extra measurements to analyze its single-particle or double-particle excitations. QSE does not require additional qubits or deeper circuits than VQE.

In most of the experimental realizations of molecular calculations on quantum computers, only small numbers of orbitals that constitute a basis of the many-electron wave function have been considered. While this is often a reasonable approximation, not including additional orbitals limits the accuracy of molecular properties, for example reaction energetics and barriers, obtained with the algorithms discussed above. The number of orbitals drives the number of qubits required and can quickly exceed those available on near-term quantum hardware. Circuit depths increase significantly with the number of orbitals as well. The virtual quantum subspace expansion (VQSE) algorithm, proposed in Ref. [17], is an extension of QSE that can include additional orbitals without the need for additional quantum resources. The authors analyzed VQSE in a numerical study and showed that it can improve accuracy of chemistry calculations. The algorithm assumes that strong correlations can be described by a subset of orbitals. Similarly to QSE, one creates the ground-state wave function using this subset on the quantum computer. VQSE then requires performing additional measurements to account for the so-called virtual orbitals that were not explicitly included in the determination of the ground-state energy, allowing one to estimate energy levels more accurately. VQSE scales polynomially with the size of the virtual orbital space.

In this work, we implement and execute the VQSE algorithm on a real quantum computer and calculate the ground-state potential energy curves of the hydrogen and lithium dimers. We find out that the noise from a quantum computer significantly impacts the generalized eigenvalue problem that needs to be solved classically and demonstrate an approach to overcome this issue. Our results show that VQSE works very well in experiments and even on imperfect and noisy quantum computers.

II. METHODS

VQSE proceeds in three steps. Firstly, we use a quantum computer to find the ground state in the active space. We do this using the VQE algorithm. Next, we measure expectation values of additional observables for the ground state. Finally, we use the measured expectation values to calculate corrections originating from the virtual space.

* urbanek@lbl.gov

A. Variational quantum subspace expansion

The electronic Hamiltonian is discretized into a finite set of orbitals. We divide the orbitals into core, active, and virtual orbitals. Core orbitals are considered frozen, i.e., these orbitals are doubly occupied and electrons in them are never excited into other orbitals. Since the Hamiltonian with frozen core orbitals can be transformed into a Hamiltonian with only active and virtual orbitals, we ignore the core space from now on. Active orbitals are the crucial part of the system because electrons in these orbitals are typically strongly correlated. Virtual orbitals give rise to corrections for quantities found by taking only the active orbitals into account.

We first create a set of expansions operators [17],

$$S = \{a_i^\dagger a_p, a_\mu^\dagger a_q a_\nu^\dagger a_r | i \in \mathcal{A} \cup \mathcal{V}; p, q, r \in \mathcal{A}; \mu, \nu \in \mathcal{V}\}, \tag{1}$$

where $a_i^\dagger$ (a_i) is the creation (annihilation) operator for an electron in spin-orbital i, and $\mathcal{A}$ and $\mathcal{V}$ are sets of active-space and virtual-space spin-orbital indices, respectively. Let $|\Psi\rangle$ be the ground-state wave function of a Hamiltonian A restricted to the active space. States $O_i|\Psi\rangle$, where $O_i \in S$, are single or double excitations of $|\Psi\rangle$. We next create a matrix A representing the unrestricted Hamiltonian in the expanded set of wave functions. A is given by its elements

$$A_{ij} = \langle\Psi|O_i H O_j|\Psi\rangle, \tag{2}$$

where $O_i, O_j \in S$. States $O_i|\Psi\rangle$ are not orthonormal. To find the energy spectrum in the expanded set, it is thus necessary to solve a generalized eigenvalue problem

$$AC = BCE, \tag{3}$$

where the overlap matrix B is given by its elements

$$B_{ij} = \langle\Psi|O_i O_j|\Psi\rangle, \tag{4}$$

C is a matrix of eigenvectors, and E is a diagonal matrix of eigenvalues.

The operators $O_i O_j$ and $O_i H O_j$ can be transformed using the Jordan–Wigner [18] or a similar transformation to qubit operators. If $|\Psi\rangle$ is the ground-state wave function created on a quantum computer, the expectation values $\langle\Psi|O_i O_j|\Psi\rangle$ and $\langle\Psi|O_i H O_j|\Psi\rangle$ correspond to expectation values of strings of Pauli operators acting on qubits. The structure of S ensures that only expectation values measured in the active space are nonzero.

B. Molecular Hamiltonian

Our goal is to find the ground-state energy of the hydrogen and lithium dimers. We represent their electronic wave functions in the cc-pVDZ basis [19]. The full molecular Hamiltonian of each molecule contains thousands of terms. We divide the Hilbert space of H_2 into an active space with two orbitals and a virtual space with eight orbitals. Similarly, we divide the space of Li_2 into a core space with two orbitals, an active space with two orbitals, and a virtual space with six orbitals.

C. Reduction to two qubits

Since our active spaces contain only two orbitals, they can be mapped to four qubits. We are targeting ground states with two electrons and zero total spin. This subspace contains only four basis states and can be mapped to two qubits [5, 8, 10]. We therefore restrict our four-qubit active-space Hamiltonian to a two-qubit Hamiltonian to further simplify the problem. We do this by projecting the Hamiltonian onto a subspace of wave functions that describe two electrons with opposite spins. The basis of this subspace is given by four-qubit states $|0011\rangle$, $|0110\rangle$, $|1001\rangle$, and $|1100\rangle$, where even and odd qubits represent spin-up and spin-down electrons, respectively. These four states are then mapped to the basis states of our two qubits. The projected Hamiltonian is given by

$$H = g_1 I + g_2 Z_1 + g_3 Z_2 + g_4 Z_1 Z_2 + g_5 Y_1 Y_2, \tag{5}$$

where coefficients g_i are calculated numerically.

D. Virtual quantum eigensolver

We use the VQE algorithm with the unitary coupled-clusters (UCC) ansatz [3, 5, 10, 20, 21] to find the ground state in the active space reduced to two qubits. The ansatz is given by

$$|\psi(\theta)\rangle = e^{-i\theta Y_1 X_2/2}|\Phi\rangle, \tag{6}$$

where Y_1 and X_2 are Pauli Y and X matrices acting on the first and second qubit, respectively, and $|\Phi\rangle = |00\rangle$ is the Hartree–Fock wave function. The wave function energy is given by

$$E(\theta) = g_1 + g_2\langle Z_1\rangle_\theta + g_3\langle Z_2\rangle_\theta + g_4\langle Z_1 Z_2\rangle_\theta + g_5\langle Y_1 Y_2\rangle_\theta, \tag{7}$$

where $\langle O\rangle_\theta = \langle\psi(\theta)|O|\psi(\theta)\rangle$. The ground state can be found by minimizing $E(\theta)$. Since ansatz (6) has one parameter only, we sweep the full domain of θ and perform the minimization during post-processing. We also measure other expectation values to estimate the elements of A and B.

E. Generalized eigenvalue problem

Energy levels of a molecule are the eigenvalues of generalized eigenvalue problem (3). Elements of the A and B matrices are linear combinations of measured expectation values. They are noisy due to imperfections of real quantum computers and also due to shot noise. A

solution of the generalized eigenvalue problem exists only if B is a positive-definite matrix. Both A and B are Hermitian indefinite matrices because they are created from noisy experimental data. The positive-definiteness of B is therefore not guaranteed. To regularize the problem, we perform an eigenvalue decomposition of B, select an optimal number of largest eigenvalues, and project both A and B onto the subspace corresponding to these eigenvalues. We then solve the generalized eigenvalue problem with the projected matrices. The number of largest eigenvalues of B that are preserved is maximized under the constraint that all of them are positive and that the projected generalized eigenvalue problem contains no spurious eigenvalues. Spurious eigenvalues are detected by computing finite differences of the lowest eigenvalue as a function of the number of preserved eigenvalues of B. We observe that the lowest eigenvalue decreases monotonically until either B becomes indefinite or a spurious eigenvalue appears. The latter case results in a sudden jump in the energy. If we selected all positive eigenvalues instead of an optimized number of eigenvalues, spurious energy levels would appear in the obtained potential energy curves.

III. RESULTS

All calculations were performed on the IBM Q Johannesburg quantum computer. Since we used two qubits only, we estimated the overall circuit fidelity from reported gate fidelities for all pair of qubits and chose the pair with the highest overall fidelity. The selected qubits were qubits Q0 and Q1.

The executed circuit is shown in Fig. 1. It creates a UCC ansatz (6) and performs a measurement in a selected basis. Each R_t gate is the I, $R_x(\pi/2)$, or $R_y(-\pi/2)$ gate for measuring a qubit in the Z, Y, or X basis, respectively. Since the ansatz depends only on a single parameter, we do not perform the VQE feedback loop to find the energy minimum. We instead sample the full domain of θ and perform the minimization on a classical computer later. In particular, we run the circuit for 257 values of $\theta \in [-\pi, \pi]$ and for all nine combinations of the R_t gates. Each individual circuit was sampled with 8192 shots. The raw data were unfolded [22] to correct readout errors [6, 9, 23]. We then calculated all two-qubits expectation values $\langle P_1 P_2 \rangle_\theta$, where $P_i \in \{I, X, Y, Z\}$ is a Pauli matrix acting on the i-th qubit. The same measured expectation values were used for both the H_2 and Li_2 molecules.

Next, we performed a separate calculation for each molecule and for each internuclear separation. The electronic wave functions were represented using the cc-pVDZ basis set. The Hamiltonian terms were calculated in OpenFermion [24] using its interface to Psi4 [25]. The molecular Hamiltonian in the active space with two orbitals was transformed using the Jordan–Wigner transformation to a four-qubit Hamiltonian and then projected to a reduced

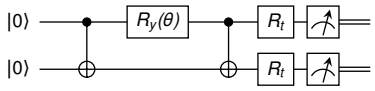

FIG. 1. A quantum circuit for the preparation of the UCC ansatz (6) and for the measurement of its expectation values. Gates R_t perform a basis transformation that depends on the measured term.

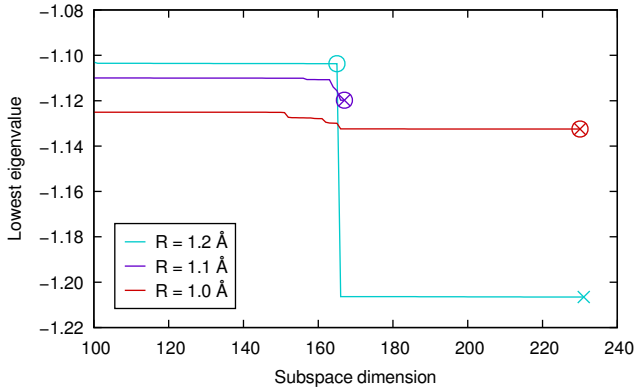

FIG. 2. Results of the eigenvalue regularization procedure for the H_2 molecule and three values of its internuclear separation R. The plot shows the lowest eigenvalue of generalized eigenvalue problem (3) as a function of the number of largest eigenvalues of the B matrix preserved in the regularization procedure. Crosses mark energies obtained when preserving all positive eigenvalues. Circles mark energies found using our regularization method.

two-qubit Hamiltonian. We then calculated and smoothed the expectation value of energy $E(\theta)$ from the measured expectation values, and then found $\theta_{\min}$ that minimized it. The minimal energy $E(\theta_{\min})$ is equivalent to the energy obtained using the VQE algorithm. All measured expectation values $\langle P_1 P_2 \rangle_\theta$ were evaluated at $\theta_{\min}$ for their use in later calculation stages.

We then created a list of expansion operators O_i. The operators that changed the total spin number or that produced a state with the norm below a cutoff when applied to the measured ground state were removed from the list. The A matrix was calculated by first transforming operators $O_i H O_j$ using the Jordan–Wigner transformation to four-qubit operators and subsequently projecting them to two-qubit operators. The expectation value of each such two-qubit operator was then estimated from the evaluated expectation values $\langle P_1 P_2 \rangle_{\theta_{\min}}$. The B matrix was created in a similar fashion.

Finally, we solved generalized eigenvalue problem (3) to obtain the ground state energy. The solutions were sensitive to regularization because both A and B matrices were created from noisy data. We therefore first performed an eigenvalue decomposition of B, selected an optimal number of largest eigenvalues, and projected both B and A onto a subspace given by the eigenvectors corresponding to the selected eigenvalues. The generalized eigenvalue

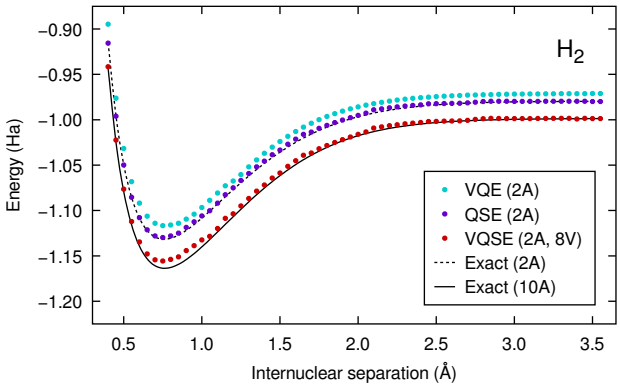

FIG. 3. Potential energy curves of the H_2 molecule in the ground state obtained using several methods. Numbers and letters in parentheses indicate the number of active (A) and virtual (V) orbitals.

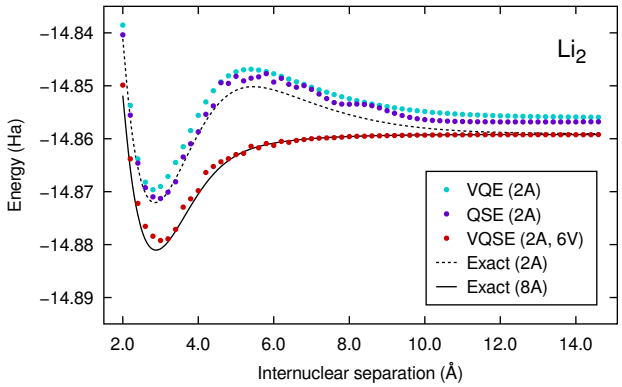

FIG. 4. Potential energy curves of the Li_2 molecule in its singlet ground state obtained using several methods. Numbers and letters in parentheses indicate the number of active (A) and virtual (V) orbitals.

problem was solved using the projected B and A matrices. Fig. 2 shows the idea behind the regularization procedure. The lowest eigenvalue evolves in a continuous way for internuclear separations $R = 1.0\,\text{Å}$ and $R = 1.1\,\text{Å}$, although the number of positive eigenvalues of B varies. For $R = 1.2\,\text{Å}$, a spurious eigenvalue appears from 166 eigenvalues onward. The optimum is therefore selected at 165 eigenvalues.

The calculations were performed both for zero virtual orbitals and the selected number of virtual orbitals. The results for zero virtual orbitals are equivalent to QSE results.

A. Hydrogen dimer

Potential energy curves for H_2 in the ground state are shown in Fig. 3. The exact solutions were found by full configuration interaction (FCI) calculations within the chosen orbital subspace. Both VQE and QSE take into account the active space only. QSE substantially improved the VQE result. VQSE takes into account both the active and virtual spaces. Executing VQSE with two active and eight virtual orbitals gave rise to 296 expansion operators. VQSE significantly improved the accuracy of the ground state energy. Its results with eight virtual orbitals are close to the exact FCI result with ten virtual orbitals. The largest difference is 9.9 mHa at $R = 0.9\,\text{Å}$. The differences from the FCI solution are caused by noise. We confirmed this by executing VQSE with data obtained from a state-vector simulator. The noiseless result matched the FCI solution.

B. Lithium dimer

Potential energy curves for Li_2 in its singlet ground state are shown in Fig. 4. Similarly to H_2, QSE improved the VQE result, but both methods take into account orbitals in the active space only. Solutions in the active space with two orbitals gave rise to an avoided crossing manifesting itself as a hump in the energy at intermediate internuclear separations. The hump is an artefact of a small active space and disappears when one takes additional orbitals into account. VQSE with two active and six virtual orbitals gave rise to 176 expansion operators. The VQSE method with two active and six virtual orbitals produced a result close to the exact FCI solution with eight active orbitals and without a hump. The largest difference is 2.5 mHa at $R = 2.6\,\text{Å}$. VQSE therefore improved the potential energy curve both qualitatively and a quantitatively in this case.

IV. CONCLUSIONS

We implemented the VQSE method proposed in Ref. [17] on the IBM Q Johannesburg quantum computer and used it to calculate the potential energy curves of the H_2 and Li_2 molecules. The noise of the quantum hardware is found to significantly impact the classical generalized eigenvalue problem and we developed a robust mathematical approach to address this issue. The obtained results show a significant improvement in accuracy over the VQE and QSE methods with the same number of qubits. In the present work, we used only two qubits to model molecules with up to ten orbitals, which would typically require twenty qubits using other algorithms. VQSE is therefore a promising method for studying chemical systems on near-term quantum computers.

ACKNOWLEDGMENTS

We thank Tyler Takeshita for helpful discussions. This work was supported by the DOE under contract DE-

AC02-05CH11231, through the Office of Advanced Scientific Computing Research (ASCR) Quantum Algorithms Team and Accelerated Research in Quantum Computing programs. This research used resources of the Oak Ridge Leadership Computing Facility, which is a DOE Office of Science User Facility supported under Contract DE-AC05-00OR22725.

[1] M. Reiher, N. Wiebe, K. M. Svore, D. Wecker, and M. Troyer, Proc. Natl. Acad. Sci. U.S.A. **114**, 7555 (2017).
[2] A. Aspuru-Guzik, A. D. Dutoi, P. J. Love, and M. Head-Gordon, Science **309**, 1704 (2005).
[3] A. Peruzzo, J. McClean, P. Shadbolt, M.-H. Yung, X.-Q. Zhou, P. J. Love, A. Aspuru-Guzik, and J. L. O'Brien, Nat. Commun. **5**, 4213 (2014).
[4] J. R. McClean, J. Romero, R. Babbush, and A. Aspuru-Guzik, New J. Phys. **18**, 023023 (2016).
[5] P. J. J. O'Malley, R. Babbush, I. D. Kivlichan, J. Romero, J. R. McClean, R. Barends, J. Kelly, P. Roushan, A. Tranter, N. Ding, B. Campbell, Y. Chen, Z. Chen, B. Chiaro, A. Dunsworth, A. G. Fowler, E. Jeffrey, E. Lucero, A. Megrant, J. Y. Mutus, M. Neeley, C. Neill, C. Quintana, D. Sank, A. Vainsencher, J. Wenner, T. C. White, P. V. Coveney, P. J. Love, H. Neven, A. Aspuru-Guzik, and J. M. Martinis, Phys. Rev. X **6**, 031007 (2016).
[6] A. Kandala, A. Mezzacapo, K. Temme, M. Takita, M. Brink, J. M. Chow, and J. M. Gambetta, Nature **549**, 242 (2017).
[7] Y. Shen, X. Zhang, S. Zhang, J.-N. Zhang, M.-H. Yung, and K. Kim, Phys. Rev. A **95**, 020501 (2017).
[8] J. I. Colless, V. V. Ramasesh, D. Dahlen, M. S. Blok, M. E. Kimchi-Schwartz, J. R. McClean, J. Carter, W. A. de Jong, and I. Siddiqi, Phys. Rev. X **8**, 011021 (2018).
[9] E. F. Dumitrescu, A. J. McCaskey, G. Hagen, G. R. Jansen, T. D. Morris, T. Papenbrock, R. C. Pooser, D. J. Dean, and P. Lougovski, Phys. Rev. Lett. **120**, 210501 (2018).
[10] C. Hempel, C. Maier, J. Romero, J. McClean, T. Monz, H. Shen, P. Jurcevic, B. P. Lanyon, P. Love, R. Babbush, A. Aspuru-Guzik, R. Blatt, and C. F. Roos, Phys. Rev. X **8**, 031022 (2018).
[11] M. Ganzhorn, D. Egger, P. Barkoutsos, P. Ollitrault, G. Salis, N. Moll, M. Roth, A. Fuhrer, P. Mueller, S. Woerner, I. Tavernelli, and S. Filipp, Phys. Rev. Appl. **11**, 044092 (2019).
[12] C. Kokail, C. Maier, R. van Bijnen, T. Brydges, M. K. Joshi, P. Jurcevic, C. A. Muschik, P. Silvi, R. Blatt, C. F. Roos, and P. Zoller, Nature **569**, 355 (2019).
[13] R. Santagati, J. Wang, A. A. Gentile, S. Paesani, N. Wiebe, J. R. McClean, S. Morley-Short, P. J. Shadbolt, D. Bonneau, J. W. Silverstone, D. P. Tew, X. Zhou, J. L. O'Brien, and M. G. Thompson, Sci. Adv. **4**, eaap9646 (2018).
[14] R. M. Parrish, E. G. Hohenstein, P. L. McMahon, and T. J. Martínez, Phys. Rev. Lett. **122**, 230401 (2019).
[15] J. R. McClean, M. E. Kimchi-Schwartz, J. Carter, and W. A. de Jong, Phys. Rev. A **95**, 042308 (2017).
[16] X. Bonet-Monroig, R. Sagastizabal, M. Singh, and T. E. O'Brien, Phys. Rev. A **98**, 062339 (2018).
[17] T. Takeshita, N. C. Rubin, Z. Jiang, E. Lee, R. Babbush, and J. R. McClean, Phys. Rev. X **10**, 011004 (2020).
[18] P. Jordan and E. Wigner, Z. Phys. **47**, 631 (1928).
[19] T. H. Dunning, J. Chem. Phys. **90**, 1007 (1989).
[20] R. J. Bartlett, S. A. Kucharski, and J. Noga, Chem. Phys. Lett. **155**, 133 (1989).
[21] A. G. Taube and R. J. Bartlett, Int. J. Quantum Chem. **106**, 3393 (2006).
[22] B. Nachman, M. Urbanek, W. A. de Jong, and C. W. Bauer, "Unfolding quantum computer readout noise," arXiv (2019), arXiv:1910.01969 [quant-ph].
[23] K. Yeter-Aydeniz, E. F. Dumitrescu, A. J. McCaskey, R. S. Bennink, R. C. Pooser, and G. Siopsis, Phys. Rev. A **99**, 032306 (2019).
[24] J. R. McClean, K. J. Sung, I. D. Kivlichan, Y. Cao, C. Dai, E. S. Fried, C. Gidney, B. Gimby, P. Gokhale, T. Häner, T. Hardikar, V. Havlíček, O. Higgott, C. Huang, J. Izaac, Z. Jiang, X. Liu, S. McArdle, M. Neeley, T. O'Brien, B. O'Gorman, I. Ozfidan, M. D. Radin, J. Romero, N. Rubin, N. P. D. Sawaya, K. Setia, S. Sim, D. S. Steiger, M. Steudtner, Q. Sun, W. Sun, D. Wang, F. Zhang, and R. Babbush, "Openfermion: The electronic structure package for quantum computers," arXiv (2017), arXiv:1710.07629 [quant-ph].
[25] R. M. Parrish, L. A. Burns, D. G. A. Smith, A. C. Simmonett, A. E. DePrince, E. G. Hohenstein, U. Bozkaya, A. Y. Sokolov, R. Di Remigio, R. M. Richard, J. F. Gonthier, A. M. James, H. R. McAlexander, A. Kumar, M. Saitow, X. Wang, B. P. Pritchard, P. Verma, H. F. Schaefer, K. Patkowski, R. A. King, E. F. Valeev, F. A. Evangelista, J. M. Turney, T. D. Crawford, and C. D. Sherrill, J. Chem. Theory Comput. **13**, 3185 (2017).